DISPERSED HYDROXYAPATITE AND MODIFIED BIOGLASS 45S5 COMPOSITES: SINTERING BEHAVIOR OF GLASS MATRIX RANGING FROM 20 TO 30 WT% IN CALCIUM OXIDE INVESTIGATION

Silva, A. C.[1,2], Parra-Silva, J. [1], Santos, S.C. [1], Setz L.F.G. [3],
Mello-Castanho, S.R.H. [1], Braga, F. J. C. [2]

[1]Instituto de Pesquisas Energéticas e Nucleares (IPEN), São Paulo (SP), Brasil
[2]Consulmat Materiais de Referência, Soluções e Serviços Ltda., São Carlos (SP), Brasil
[3]Universidade Federal do ABC, Av. dos Estados, 5001;Santo André, SP, Brasil

e-mail: dasilva.ac@uol.com.br

Abstract*. Biomaterial technology plays an important role in cell-based tissue proliferation environment creation. The hydroxyapatite (HA) bioceramics are reference materials to employment as a bone substitute, however, their slow rate of degradation and its low rate of bioactivity (Ib) are presented as limiting factors for application as bone graft. In contrast, the bioglass (BG) is a resorbable and osteoinductive material and can act as fluxing in HA/BG composites. The present work objective the development of HA/BG (40/70wt%) composites, Three compositions of the 45S5 bioglass derived ranging from 20-30wt% in CaO were used in order to study the sintering behavior of these materials with hydroxyapatite 30wt% dispersed. The composites were uniaxially pressed in the form of cylinders and sintrerized at (1100°C/1h). The characterization was made employing scanning electron microscopy, Infra-Red Spectrometry, X-ray diffraction and hydrolytic resistance test. The results indicate the potential use of the materials developed for applications like bone graft.*
Keywords: Hydroxyapatite, Biomaterials, composite, bioglass

1.Introduction

The bioceramics are obtained and processed to provide specific physiological behavior for applications as bone grafts. bioceramics should be resorbable, thus acting as temporary material, gradually being replaced by new bone [(1,2,4)].

The hydroxyapatite (HA), a calcium phosphate bioceramic, is the main material for applications in bone replacement because it is a material that exhibits absence of local and systemic toxicity, absence of inflammatory responses and apparent ability to bind to host tissue. However, despite their promising biological properties, its low rate of bioactivity index (Ib) and its slow rate of degradation is presented as limiting factors for its application as bone graft [(5)].

Unlike HA, the bioglass is a resorbable biomaterial which has a high Ib, and osteoinductive propriety, which allows intracellular and extracellular interface response occurs in the living tissue, allowing the surface to be colonized by stem-cells free as result of surgical interventions.

In this context, in previous work the authors was compared the use of bovine bone HA with synthetic HA (calcium triphosphate) in silicate-phosphate bioglass (45S5) with HA dispersed composites (1), seeking to combine the osteoconductive and osteoinductive properties of both materials, resulting in a biomaterial with properties

suitable for application as bone grafts. As result, the best sintering behavior was reached with HA/BG relation are 40/60 wt%, and was observed too that the Bovine HA β-TCB degradation during the sintering when dispersed in the bioglass. In HA/Bioglass composites the presence of β-TCP in the composites is presented as an advantage because it is a resorbable apatite phase and with biological interest, in this way the use of synthetic HA is is more appropriate.

In this context, the present work objective was to improve HA/BG composite processing and characteristics as bone grafts, through the sinterization behavior synthetic HA (calcium triphosphate) dispersed in 45S5 bioglass variations study. The used modificated 45S5 bioglass compositios were obtained with 20, 25 and 30 wt% CaO content.

2. Experimental Procedure

2.1 Modified 45S5 Bioglass obtention

For this study we considered three bioglasses compositions with different contents of CaO in it's composition, i.e, an 45S5 traditional bioglass[6] approximate composition **containing 25wt% of CaO, and two more, one containing 20wt% of CaO and another** containing 30wt% of CaO, being denominated respectively B25, B20 and B30, in accordance with its content of calcium oxide. The oxide composition of bioglasses is described in Table I.

Table I – Calculated bioglass compositions (oxides wt%).

	SiO_2	Na_2O	CaO	P_2O_5
B20	50,29	26,05	19,08	4,58
B25	45,00	25,75	23,58	5,66
B30	39,83	25,47	27,99	6,72

The bioglasses composition were prepared using analytical grade reagents and fused at 1500 ° C for 2 hours in vertical kiln. The bioglass were quenching and cast in 10x10x50 mm bars. The annealing was performed at 500°C for 2 h, and part of the material was milled to powder (≤ 250μm).

2.2 hydroxyapatite

The synthetic hydroxyapatite ($Ca_2(PO_4)_3OH$), with high purity (99 wt%) for use in bone implants was used. These materials was kindly provided by the company Critéria Ltda.

2.3 Hidroxyapatite/Bioglass composites obtention

The raw materials were milled to fine powder (60 mesh - ≤ 250μm) and the composites were formulated in HA/BG proportions of 40/70 wt%. The samples are identified by HB followed by bioglass CaO mass proportions, i.e., HB20, HB25 and HB30. The homogenization was performed in agate mortar. For each composition five 5.0 mm in diameter cylinder test were (approximately 0.2 g of material) uniaxially compacted (1000Kgf loaded). The sintering of the green cylinders arranged in zirconia

navicular crucible was held in muffle type furnace at 1100 ° C for 2 h with 15°C /min heating rate and following natural cooling inside the oven.

2.4 Samples characterization

The composites characterization was performed using the techniques of X-ray diffraction (XRD) for powdered samples (Bruker AXS D8 Advance, USA). The measurements of the infrared spectra were performed using Thermo Nicolet - Nexus 870 FT-IR spectrometer. USA, for powdered samples (dispersion in KBr pellets, spectrophotometric grade - Merck PA). The scanning electron microscopy - SEM were performed using Hitachi T3000 aparatus (Japan). The chemical resistance evaluation (hydrolytic resistance test) was performed as described by Day [7].

3. Results and Discussion

The obtained glass FTIR spectra are showed in Fig. 1.

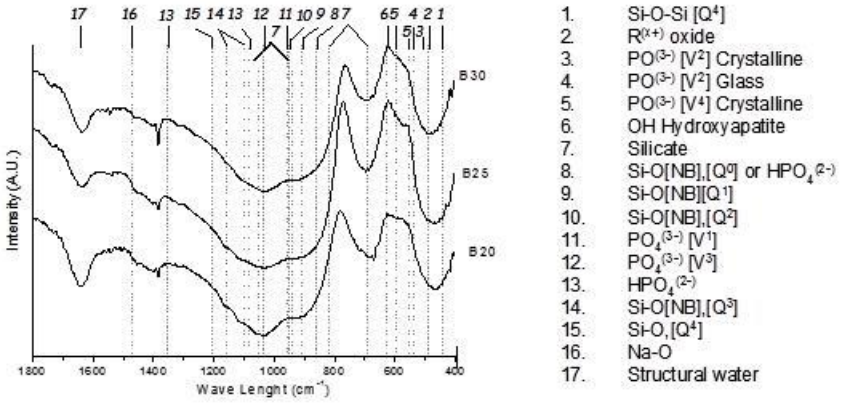

Figure 1 - FTIR spectra corresponding to B20, B25 and B30 bioglasses.

Analyzing these FTIR spectra, it can be seen a broad distribution of Q^x species in the silica amorphous network ranging from Q^4 to Q^0, especially for Q^3 and Q^2 species, showing a typical configuration of a glass soda lime (CaO: Na_2O: P_2O_5 system) of the glass which differ only by the addition of about 6 wt% of P_2O_5. This concentration in Q2 and Q3 species is shown more clearly in the spectra for the B20 bio glass.

In Fig. 1 spectra can still be observed that the indicative peaks of $PO^{(3-)}$ V^2 and V^4 groups linkages, in both crystalline and glassy forms, become better defined with the concentration of CaO in the glass, i.e, from B20 to B30 glass. However in all bioglass were observed R^{X+} segregated groups, which may be either alkali metals, alkaline earth metals or phosphate groups. However the peaks indicated of Group $PO_4^{(3-)}$ V^3 linkages with randon network are well defined by B20 bioglass, indicating a clear glassy network participation. In B25 and B30 glasses these peaks are diffuse, indicating $PO_4^{(3-)}$ group difficulty to join with glassy network. These results are consistent with the lower concentration of CaO in the glass B20, because CaO competes with SiO_2 groups by associate with the phosphate groups. In consequence, the glass B20 will probably have lower liquid phase formation temperature and lower chemical resistance than the other studied glasses.

The developed composites XRD patterns are show in Fig. 2, (green) and Fig. 3 (Sintered samples). In these diffractograms is possible to observe changes crystalline

materials characteristic for all HA/Bioglass composite, showing that the sintering period was sufficient for the occurrence of the evolution of crystalline phases.

The composites shows peaks relating to the HA and tricalcium phosphate (β-TCP) characteristic peaks, and glassy amorphous phase In general way, the peaks for TCP, are better defined for the composites obtained after sinterization. These results are HA degradation to β-TCP sintering effect indicative.

The presence of β-TCP has become the object of interest in the area of biomaterials due to their behavior resorbable. The use of b-TCP with the HA has been a viable alternative to increase the speed of assimilation of the latter [5].

In despite the Na_2O peak presence, there are no indication of bioglass devitrification during the termal treatment (sintering).

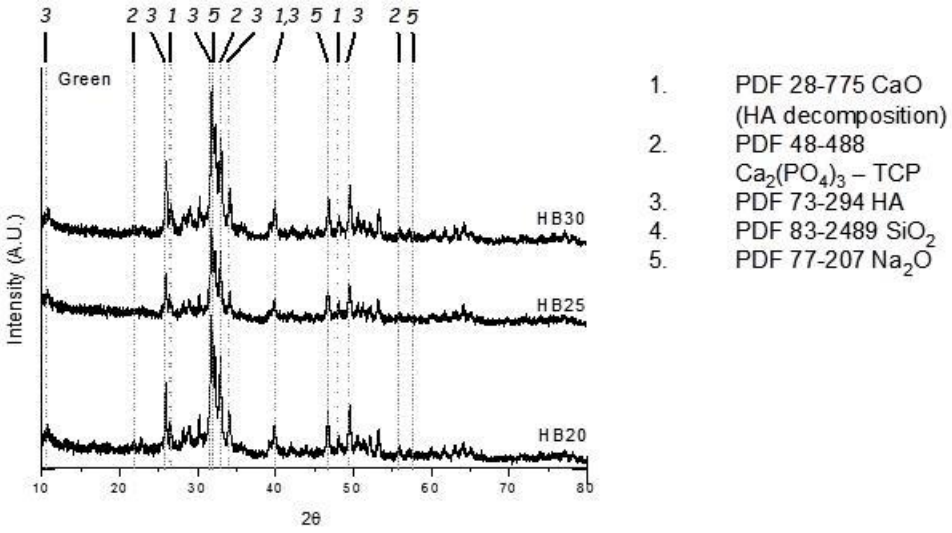

Figure 2 - XRD patterns corresponding to *HB20, HB25 and HB30 green composites*

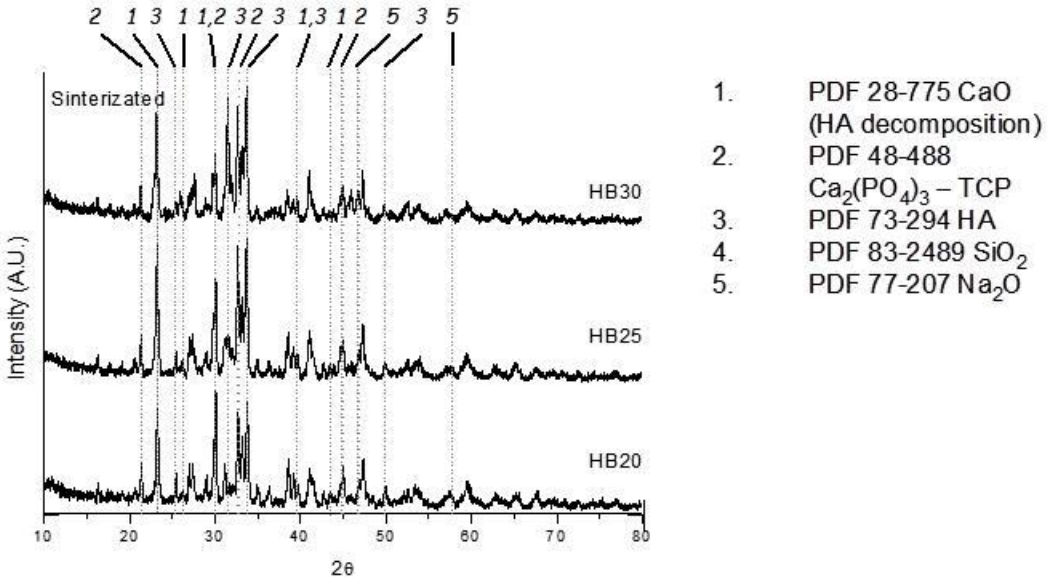

Figure 3 - XRD patterns corresponding to *HB20, HB25 and HB30 sintered composites*

The FTIR spectra for composites HB20, HB25 and HB30 in green and sintered are show in fig. 4,5 and 6 respectivaly.

In these figures, in general way in green composites spectra the hydroxyapatite spectra is overlapped with the glass spectra in between 450 cm -1 and 1000 cm-1 region. In these spectra it is possible to observe a displacement in the hidroxiapatia hydroxyl linkage indicative peak and $PO^{(3-)}$ groups (V^2 and V^4) linkages indicative peak. The displacement of these peaks may indicate an hydroxyapatite structural arrangements variation range. When green composites spectra are compareted with those of sintered composites, it is not possible to observe changes in the structure of both conposite constitutive materials as a result of sintering, as exception SiO_2 Q^1 indicative peak better definition in HB20 and HB25 composites. This result is not compatible with bioglass devitrification during sintering, and thus may indicate phosphate-silicate compounds possible formation as result HA decomposition observed by X-ray diffraction (Fig. 3).

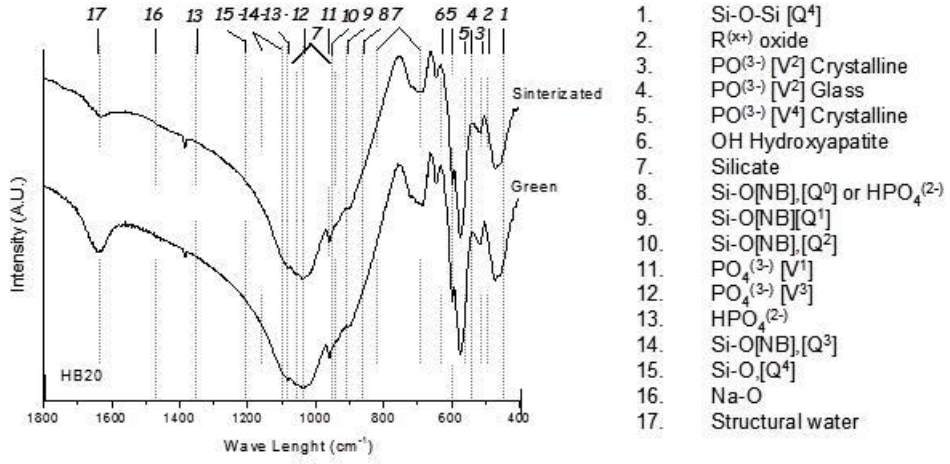

Figure 4 - FTIR spectra corresponding to HB20 composite (green and sintered)

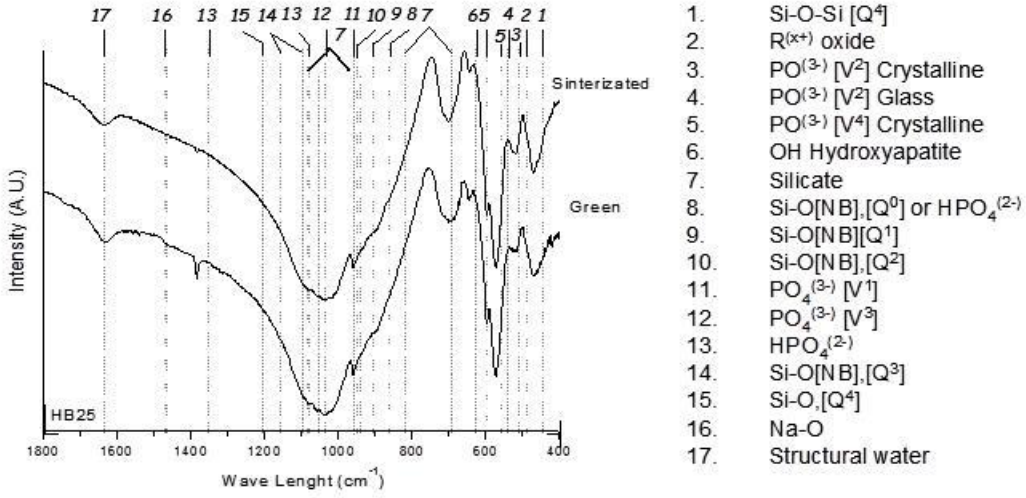

Figure 5 - FTIR spectra corresponding to HB25 composite (green and sintered)

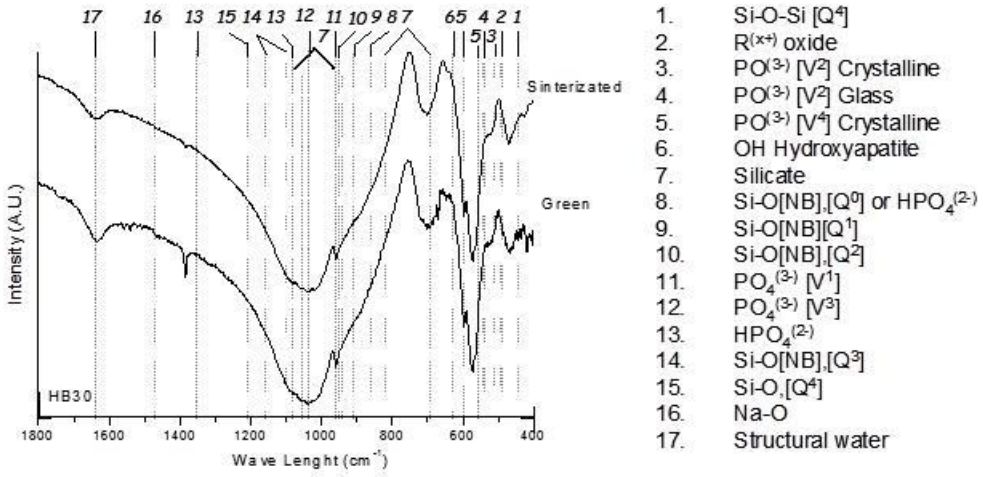

Figure 6 - FTIR spectra corresponding to HB30 composite (green and sintered)

The FB20, HB25 and HB30 SEM micrographs of the syntherized material are showed in Fig. 7-a, b & c respectily.

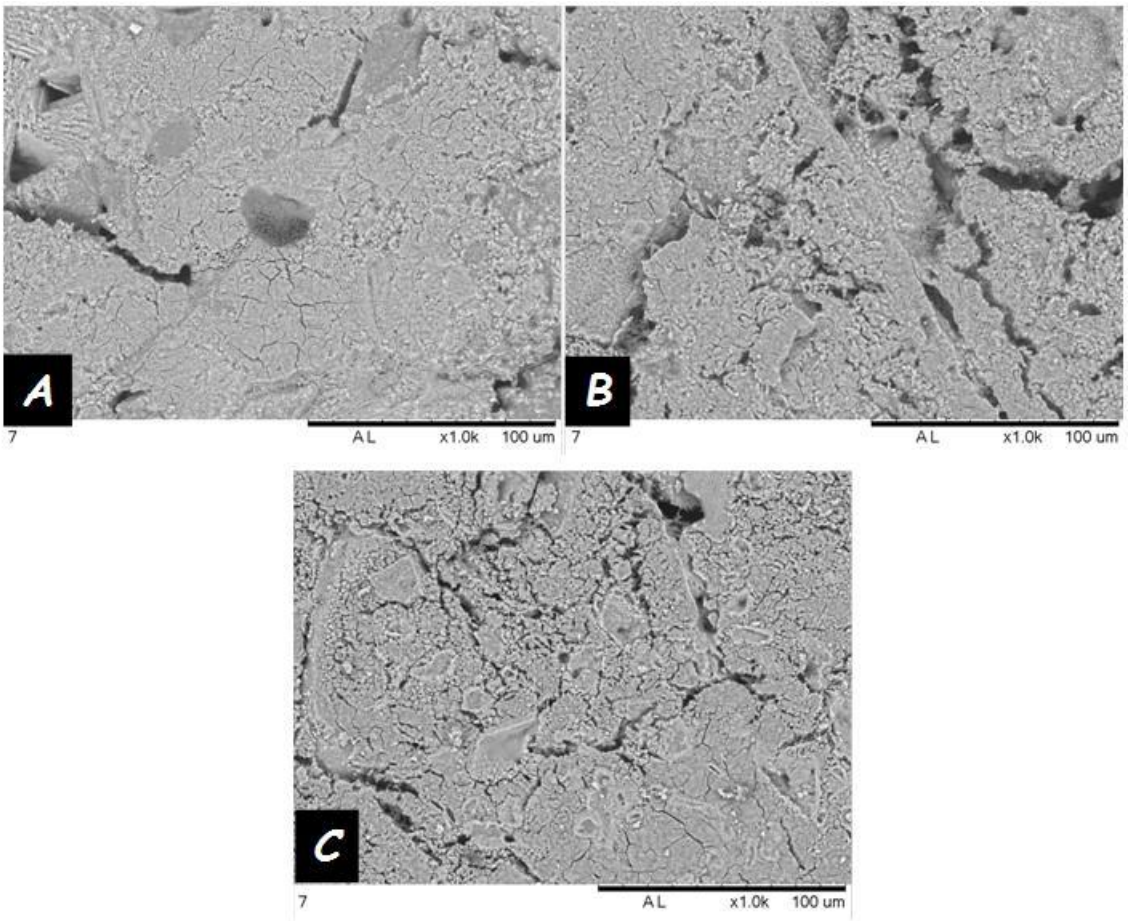

Figure 7 - SEM Micrography corresponding to: a) HB20 composite (sintered); b) HB25 composite (sintered); and, c) HB25 composite (sintered)

In these micrographs it is possible to observe the composite precursor powders densification by sintering and HA particles were effectively wetted by all bioglasses. This behavior seems to be proportional to the amount of CaO contained in the glass, i.e, HB20 composite HA particles bioglass wetting appears be more effective than that observed in HB30 composite. However, the HA particles bioglass wetting still unsatisfactory for all bioglasses (B20, B25 and B30). These results are indicating that lower liquid formation temperature are needed (modified 45S5 bioglass). In composites micrographs were also observed cracks formation after cooling.

The composites were also evaluated as to their chemical resistance through the hidrolítco attack resistance test, to allow the study of these materials dissolution kinetics. The HB20, HB25 and HB30 composite XRD patterns after 0 day and 14 days of hydrolytic attack for are showed in Fig. 8,9 and 10 respectively.

In these figures difractograms are not observed significative changes in mais peaks, for all samples. As exception are observed tre increese of Na_2O representative peaks (associeted to glass fase), and CaO representative peaks. This kind of result are indicative that proprably the glassy phase dissolution process is homogeneous (surface corrosion) with formation of a silica depleted surface layer (depleted in alkali) that comes off the surface as effect of attack intensity, exposing a new virgin glass layer, which will be etched resulting in a new silica depleted surface layer that eventually give off, in a continuous wear process. With the erosion of the glass phase, the HA phase composed by particles and surface near located, will have no mechanical support and thus leave the bulk being removed to the etching solution. It should be noted that during the hydrolytic attack does not occur material redeposition on sample surface as in simulated body fluid tests (SBF), thereby enabling identify the dominant dissolution process without bioactivity process interference.

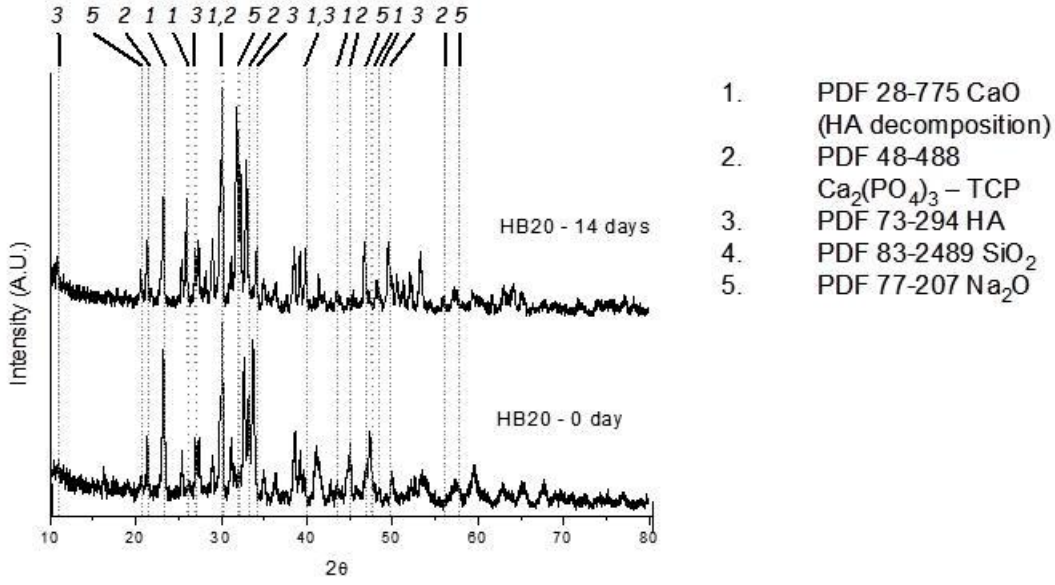

Figure 8 - XRD patterns corresponding to *HB20 sintered composites after* after 0 day and 14 days of hydrolytic attack

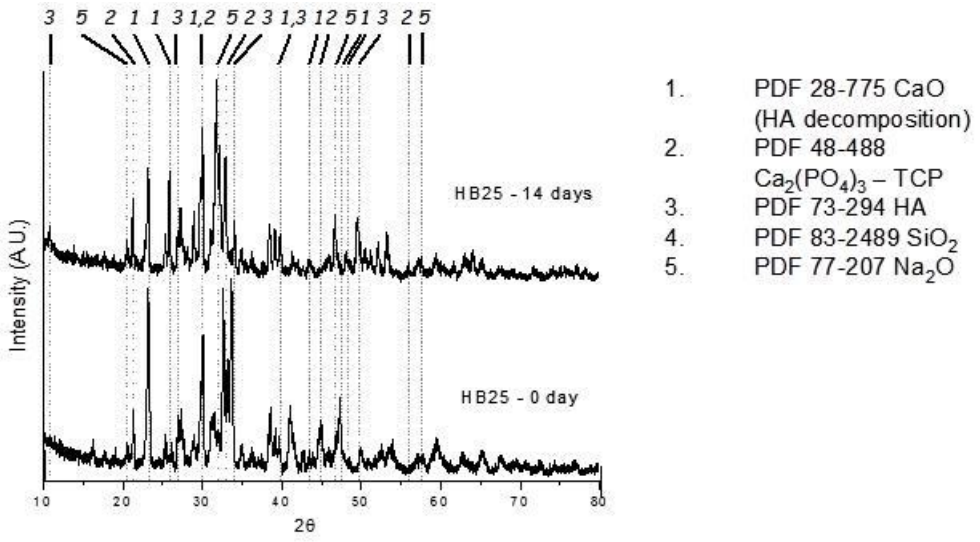

Figure 9- XRD patterns corresponding to *HB25 sintered composites after* after 0 day and 14 days of hydrolytic attack

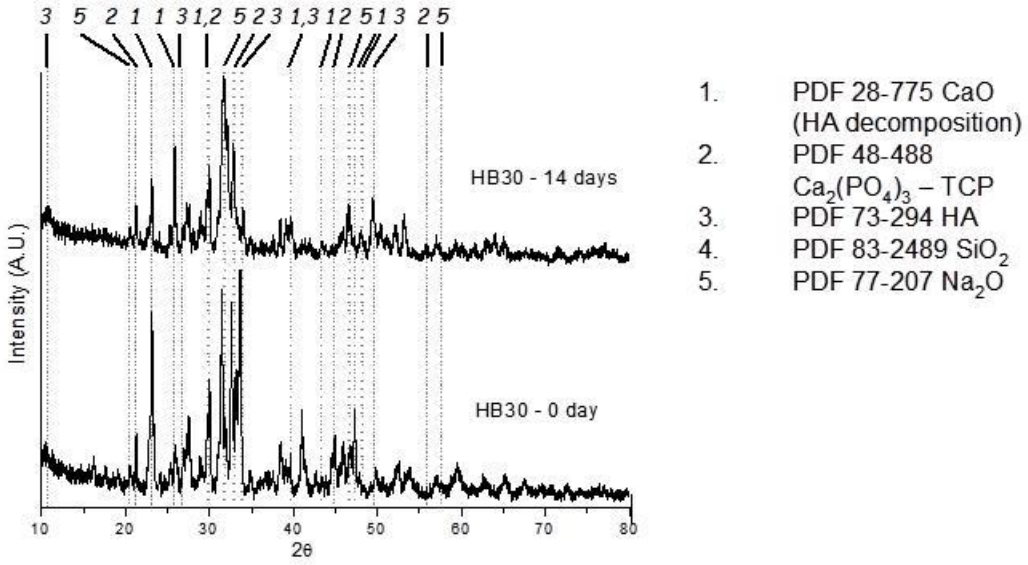

Figure 10 - XRD patterns corresponding to *HB30 sintered composites after* after 0 day and 14 days of hydrolytic attack

The Fig. 11, 12 and 13 show the FTIR spectra of the composite HB20, HB25 and HB30, after being subjected to 0, 1, 3, 7 and 14 days of hydrolytic attack.

Analyzing these FTIR spectra, it can be observe for all composite that bioglass Q^x species distribution initially concentrated in Q^3 and Q^2 (as observed in Fig. 1 FTIR spectra) tends already on the hydrolytic attack first day to an Q^3 groups favorable structural distribution equilibrium. This result is consistent with a homogeneous surface dissolution process , where Q^2 groups, make linkages with two groups R^{X+} (alkaline metals, alkaline earth metals or phosphate groups) react more easily with H^+ and OH^- cations resulting in silanol groups formation which are finally moved to the etching solution. With hydrolytic attack evolution the Q^3 species linkages indicative peak became better defined for HB20

composite spectra (HB20 composite contains B20 bioglass) indicating a lower resistance to dissolution, eg, shows a higher reactivity. In general way bioglass properties such as chemical resistance, melting temperature and softening temperature are directly proportional and structural arrangement dependent. Thus, this result may be indicative that B20 glass has better HA particles wetting ability during composite sintering.

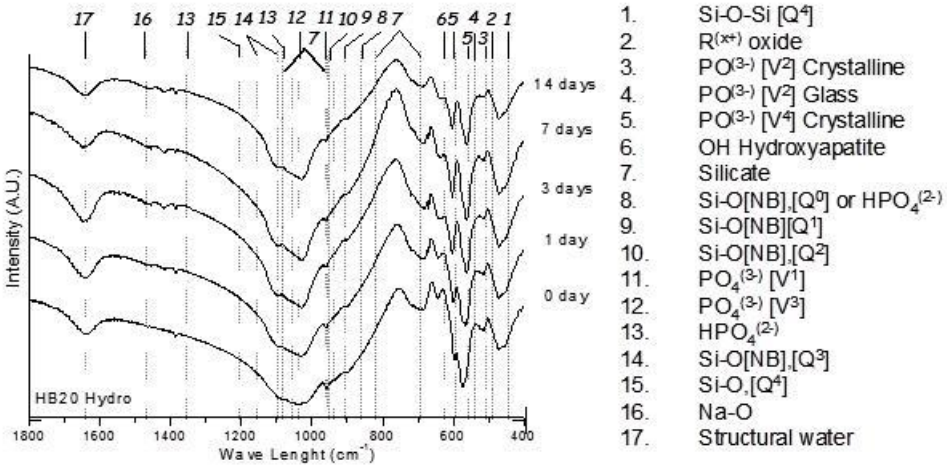

Figure 11- FTIR spectra corresponding to *HB20 sintered composites after* after 0, 1, 3, 7 and 14 days of hydrolytic attack

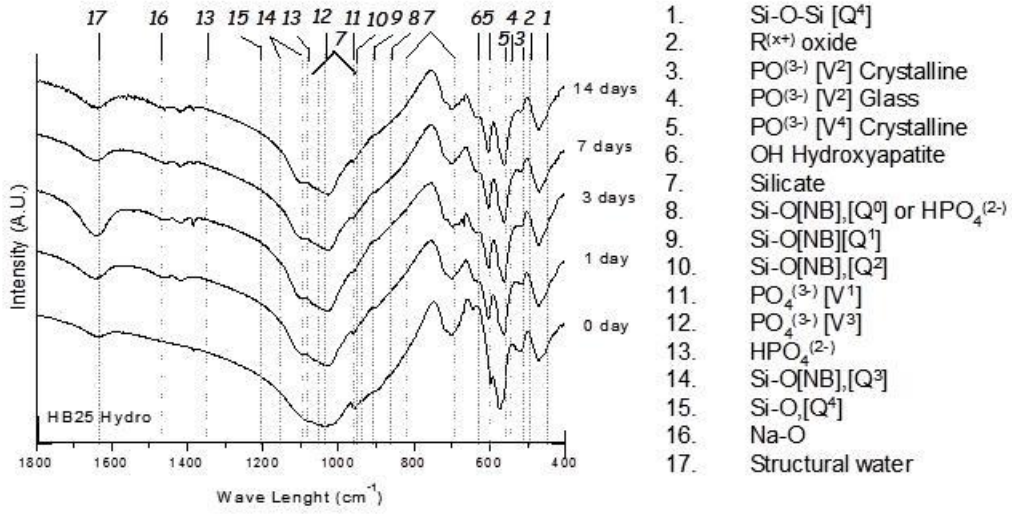

Figure 12- FTIR spectra corresponding to *HB25 sintered composites after* after 0, 1, 3, 7 and 14 days of hydrolytic attack

In the spectra represented in the figures, can also observe that the indicative of crystallyne $PO^{(3-)}$ V^2 groups linkage peaks definition decreased in etching time dependence, steadily for the HB20 (Fig. 11) while for the other composites, i.e, HB25 and HB30 (figs. 12 and 13 respectively) only in hydrolytic attack first day changes are observed. In the $PO_4^{(3-)}$ V^2 group amorphous linkages with randon network peaks indicative are observed a sharpening only 14 days hydrolytic attack for the HB20 composite,

approximately in a half of the etching time for the HB25 composite and in the first day for the HB25 composite, this behavior assigned a phosphate groups retention at bioglass surface layer, as a result of different dissolution rates en function of each glass CaO content. It is important to clarify that this phenomenon is not relacionated with bioactivity, as this is of bioglass surface cations redeposition dependent it which is deliberately prevented in test procedure used. In the of $PO_4^{(3-)}$ V^4 group linkages peaks indicative in the FTIR spectra of all composites en two phenomena are observed according to the hydrolytic attack time: i) identifying those peaks increases sharply, and ii) the displacement of these peaks (observed in Fig. 4, 5 and 6 FTIR spectra) is fixed. A similar effect is observed on OH group of hydroxyapatite indicative peaks, however in this specific case, the intensity of the peaks is reduced to the composite spectra of HB30. These results are for all bioglass compositions indicate of HA particles surface wetting occurrence. Thus, the HA particles were encapsulated and protected from wear while bioglass was not corroded. In accordance with the dissolution rate of each bioglass, HA encapsulated particles were exposed to the etching solution and might react, so that the HA reactivity is controlled by the used bioglass. Could not confirm yet if there chemical reactions between the bioglass and HA, but the possibility should be considered for this bioglasses more soluble.

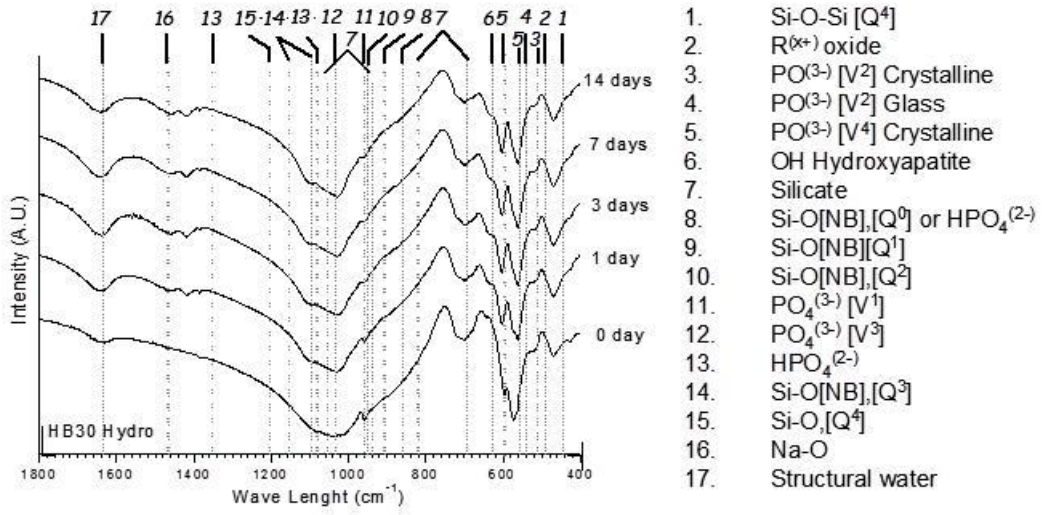

Figure 13- FTIR spectra corresponding to *HB30 sintered composites after* after 0, 1, 3, 7 and 14 days of hydrolytic attack

The comparison of SEM micrographs of composites after 14 days hydrolytic attack (Figs. 14-a, b & d) indicate the superficial dissolution of the bioglass phase in all samples, however, the dissolution was more intense in the composite HB20, leaving HA crystals exposed on surface. These results are in agreement with the results obtained by other methods and confirm the previous discussion. Thus, when implanted in living organism, the dissolution of bioglass and also the β-TCP, which is resorbable, will lead to formation of a surface with many calciun phosfate derivated materials. The formed surface will receive a response in the intracellular and extracellular interface with living tissue enabling them to be colonized by stem cells free, due to the osteoinductive character of bioglass. It is hoped that with the glassy phase and β-TCP phase dissolution

progress the bone tissue formed involving the HA particles remnants and interacting with they as result of HA osteoconductive character.

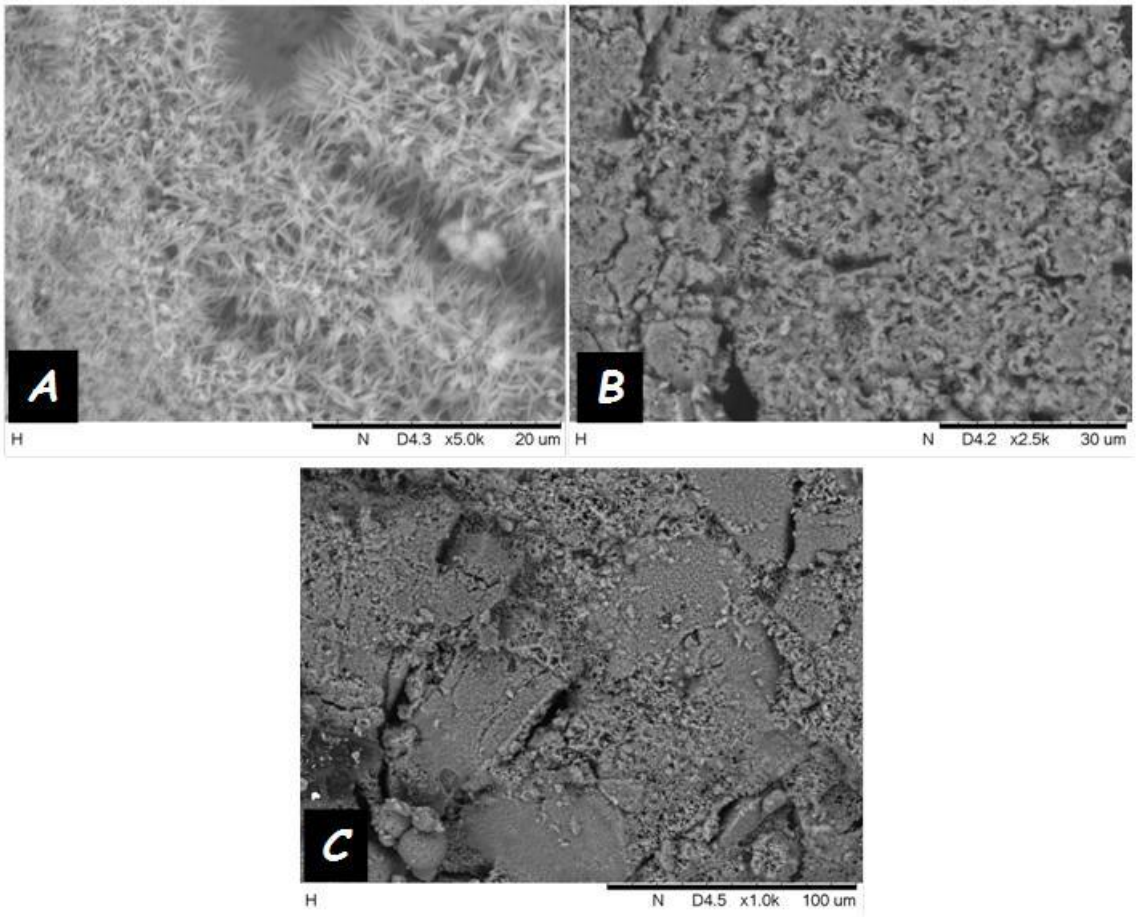

Figure 14- SEM micrographies after 14 days hydrolytic attack: a) HB20; b) HB25; and, HB30

4. Conclusions

The addition of synthetic HA to the bioglass was able to produce potentially resorbable composites, which will allow the combintion of osteoconductive and osteoinductive properties of the each materials. for this purpose the us of a improved sintering characteristics modified bioglass viability was demonstrated. In this initial study the hydroxyapatite wettability by bioglass and bioglass effect in hydroxyapatite reactivity was indicatated. In tested bioglasses the modification of the classical 45S5 bioglass with the reduction of its calcium content of 5 wt% showed the best behavior. From these results it is possible the development of new bio glass intended for use in HA / bioglass composite where the interest properties of both materials can be combined resulting in appropriate biomaterials for bone graft.

Acknowledgments
The authors would like to acknowledge the financial support and scholarships from Capes/Finep project PNPD/FINEP n.º 2462095 and to Fapesp, projects: 96/09604-9, 99/01924-2 & 0002483-9.

References:

1. HENCH, L.L. Bioceramics: from concept to clinic. **J. Am. Ceram. Soc**. v.74, p.1,487 1991.
2. HENCH, L.L. WILSON, J. An introduction to bioceramics, in: Advanced Series in Ceramics, vol I, World Scientific, London, 1993.
4. HENCH, L.L. CAO, W. Bioactive Materials, **J. Ceram. Int.** v.22, p. 493,1996.
5. GUASTALDI, A. C. APARECIDA, A. H. Fosfatos de cálcio de interesse biológico: importância como biomateriais, propriedades e métodos de obtenção de recobrimentos. **Química Nova**, v.33, p. 1352, 2010.
6. Li, D. YANG, M.X. MURALIDHA, WUB, C. YANG, F. Local surface damage and material dissolution in 45S5 bioactive glass: Effect of the contact deformation **Jour. of Non-Cryst. Solids**, v.355, p. 874, 2009.
7. DAY, D.E. WU, Z. RAY, C.S. HRMA, P. Chemically durable iron phosphate glass waste forms, **J. Non-Cryst. Solids**, v.241, p.1–12, 1998.